Precision QCD with heavy quark production

Sasha Zenaiev
(Hamburg University)

Overview:

$c\bar{c}$, $b\bar{b}$ @ HERA ep $\rightarrow$ m_c, m_b, PDFs

Eur. Phys. J. C78 (2018) 473

$c\bar{c}$, $b\bar{b}$ @ LHC pp $\rightarrow$ PDFs, cosmic rays

Eur. Phys. J. C75 (2015) 396 JHEP05 (2017) 004 JHEP04 (2020) 118

$t\bar{t}$ @ LHC pp $\rightarrow$ m_t, α_S, PDFs

Eur. Phys. J. C80 (2020) 658 JHEP04 (2021) 043 Garzelli, Mazzitelli, Moch, Zenaiev, in preparation

Theory Challenges in the Precision Era of the Large Hadron Collider
Florence, Italy
28 August 2023

What is interesting in heavy quark (HQ) production?

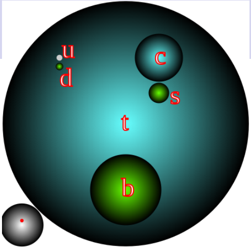

- $m_c, m_b, m_t > \Lambda_{\mathrm{QCD}}$ provides a hard scale
  - pQCD benchmark (LO, NLO, aNNLO, NNLO. . .)
- Different HQ masses (1.3 . . . 170 GeV)
  - different impact of radiative corrections and non-perturbative effects
  - $m_c \approx$ 1.3 GeV: fragmentation effects are important
  - $m_t \approx$ 170 GeV: excellent test of pQCD convergence
- Probe of **proton structure,** e.g. $gg \to t\bar{t}$, $gs \to Wc$ etc.
- Production sensitive to **α_s and HQ masses**
  - extraction of **fundamental SM parameters**
- May provide insight into possible new physics

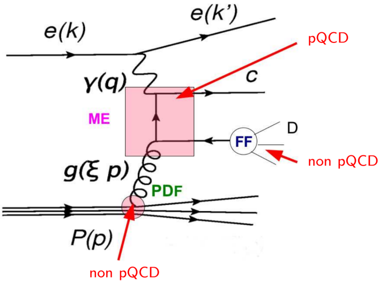

$$\sigma = \mathbf{PDF} \otimes \mathbf{ME} \otimes \mathbf{FF}$$

Combined HERA charm and beauty data [Eur. Phys. J. C78 (2018) 473]

- legacy data on charm and beauty production from HERA
- enable **precise** determination of charm and beauty $\overline{\mathrm{MS}}$ masses
- reveal tension in describing simultaneously HQ and inclusive HERA data

$$m_c(m_c) = 1290^{+46}_{-41}(\mathrm{fit})^{+62}_{-14}(\mathrm{mod})^{+3}_{-31}(\mathrm{par})\ \mathrm{MeV}$$

$$m_b(m_b) = 4049^{+104}_{-109}(\mathrm{fit})^{+90}_{-32}(\mathrm{mod})^{+1}_{-31}(\mathrm{par})\ \mathrm{MeV}$$

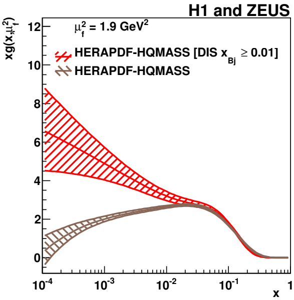

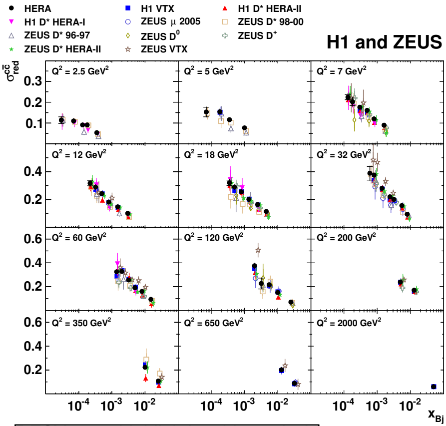

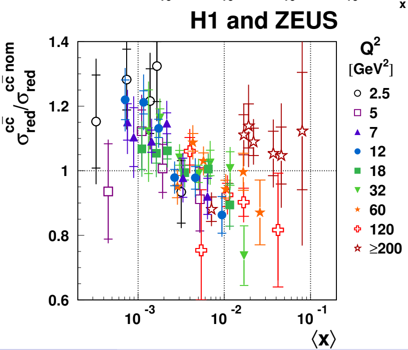

DESY news highlighting this analysis

Charm production at LHC → gluon at low x → atmosphere ν fluxes

- LHCb measured:
  - charm $0 < p_T < 8$ GeV, $2 < y < 2.5$ [NPB871 (2013) 1]
  - beauty $0 < p_T < 40$ GeV, $2 < y < 2.5$ [JHEP 1308 (2013) 117]
- First QCD analysis of these data: Eur. Phys. J. C75 (2015) 396
- Improved gluon and sea-quark distributions up to $x \gtrsim 5 \times 10^{-6}$ (not covered by other experimental data)
  - used in next paper to predict IceCube background for very high energy cosmic ν [JHEP05 (2017) 004]
  - further update with ALICE and new LHCb data [JHEP04 (2020) 118]

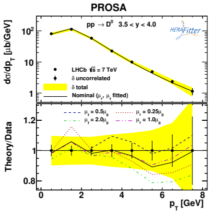

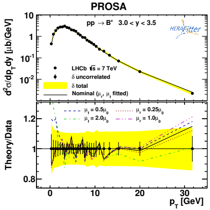

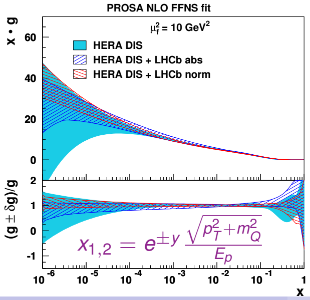

⇒

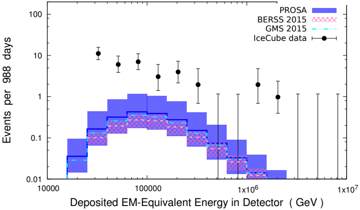

Charm production at LHC: dealing with large NLO scale variation uncertainties

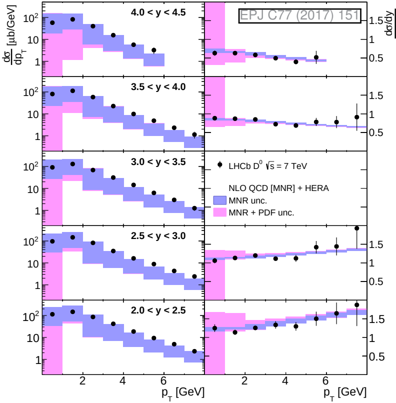

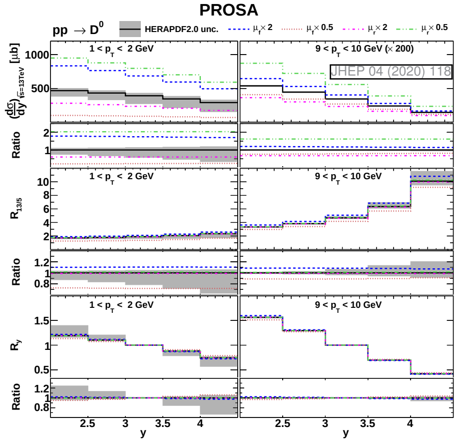

- Taking **ratios** of data → reducing scale uncertainties by one order of magnitude
- Ratio to another kinematic region might be better than (traditional) ratio to another c.m.e.
- This relies on assumption that scale unc. are correlated across different kinematic regions:
  - can be tested e.g. by using another (dynamical) scale choice

Why measure $t\bar{t}$ production?

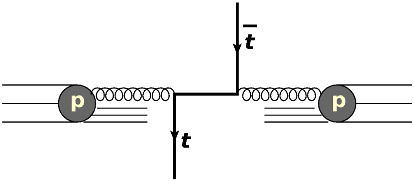

- m_t provides a hard scale
  ⇒ ultimate probe of pQCD
  (NLO, aNNLO, NNLO, ...)
- Produced mainly via *gg*
  ⇒ constrain gluon PDF at high x
- Production sensitive to α_s and m_t^{pole}
- May provide insight into possible new physics

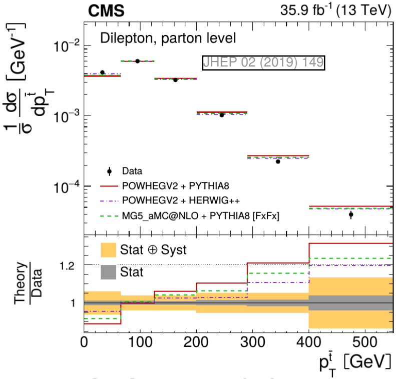

Why measure 2D/3D?

- Previous 1D measurements: overall good agreement, but reveal some trends
- 2D: study production dynamics in more detail
  EPJ C77 (2017) 459
- **3D:** simultaneously constrain α_s, m_t^{pole}, PDF
  EPJ C80 (2020) 658

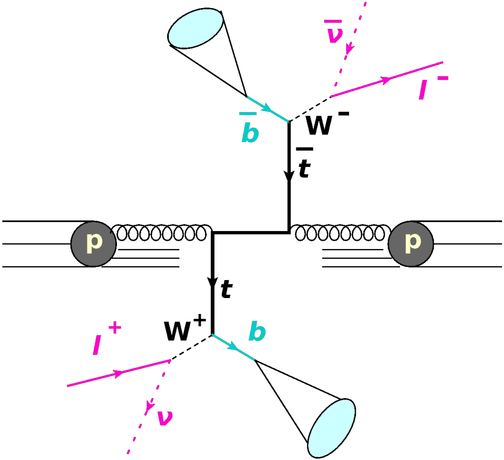

Follows 1D measurement:

- **Leptons:**
  - 2 isolated $l^{\pm}l^{\mp}$
  - $p_T > 20(25)$ GeV
  - $|\eta| < 2.4$
- **Jets:**
  - at least 2 jets
  - $p_T > 30$ GeV
  - $|\eta| < 2.4$
  - at least 1 *b*-tagged

Kinematic reconstruction:

(1) **Full reconstruction:**
  - reconstruct t, $\bar{t}$
  - use all constraints

(2) **Loose reconstruction (NEW):**
  - reconstruct $t\bar{t}$
  - m_t constraints not used

  $\rightarrow$ essential for m_t^{pole} extraction

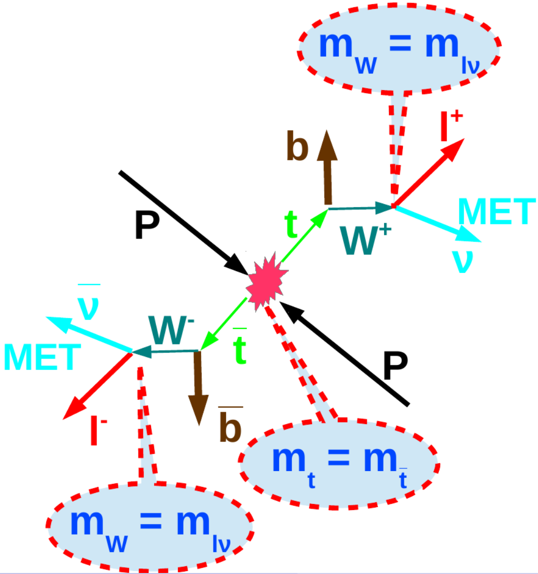

- Measured input: leptons, jets, MET
- Unknowns: $\bar{p}_{\nu}$, $\bar{p}_{\bar{\nu}}$ (6)
- Constraints:
  - m_t, $m_{\bar{t}}$ (2)
  - m_{W^+}, m_{W^-} (2)
  - $(\bar{p}_{\nu} + \bar{p}_{\bar{\nu}})_T = \mathrm{MET}$ (2)

Two variants:

(1) Full reconstruction:

- reconstruct t, $\bar{t}$
- use all constraints

(2) Loose reconstruction:

- reconstruct $t\bar{t}$ (4 unknowns)
- m_t constraints not used
  $\rightarrow$ reliable for M_{T} extraction

Side remark:

- experimentally, it is easier to measure $t\bar{t}$ rather than t or $\bar{t}$ (at least in the dilepton channel)

Overview of measured cross sections

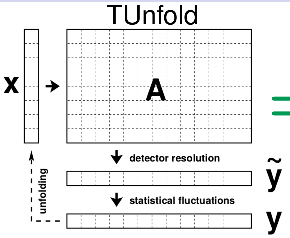

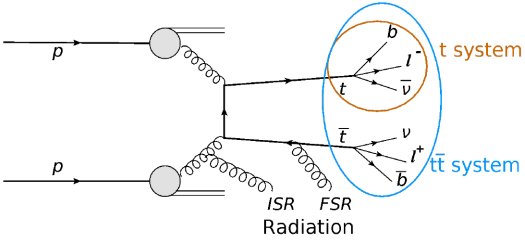

- ***t* production:**
  - [$y(t)$,$p_T(t)$]: most "simple"
- **$t\bar{t}$ production:**
  - [$M(t\bar{t})$,$y(t\bar{t})$]: most sensitive to PDFs (at LO $x_{1,2} = \sqrt{\frac{M(t\bar{t})}{s}} e^{\pm y(t\bar{t})}$)
  - [$M(t\bar{t})$,$p_T(t\bar{t})$]: sensitive to radiation
- **t, $t\bar{t}$ mixed:**
  - [$M(t\bar{t})$,$y(t)$]: sensitive to PDFs
  - [$M(t\bar{t})$,$\Delta\phi(t,\bar{t})$]: sensitive to radiation
  - [$M(t\bar{t})$,$\Delta\eta(t,\bar{t})$]: shed further light on $p_T(t)$ problem
- **NEW $t\bar{t}$ production with extra jets:**
  - [$N_{\text{jet}}^{0,1+}$,$M(t\bar{t})$,$y(t\bar{t})$]: sensitive to α_s, m_t^{pole} and PDFs (nominal extraction)
  - [$N_{\text{jet}}^{0,1,2+}$,$M(t\bar{t})$,$y(t\bar{t})$]: sensitive to α_s, m_t^{pole} and PDFs (cross check)

Results: $[N_{\text{jet}}^{0,1+}, M(t\bar{t}), y(t\bar{t})]$ compared to NLO pred. with diff. PDFs

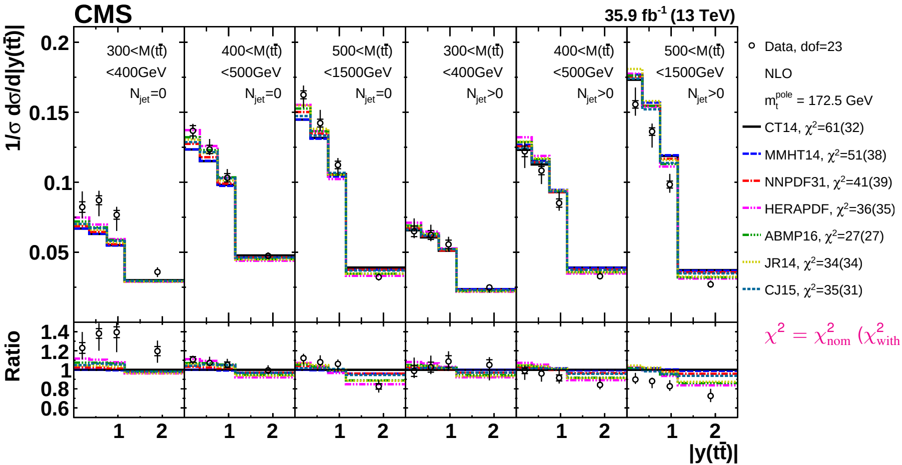

$\chi^2 = \chi^2_{\text{nom}}\ (\chi^2_{\text{with PDF unc.}})$

- description depends on PDFs → data are sensitive to PDFs
- all modern PDF sets considered
  - best description given by ABMP16

Results: $[N_{\text{jet}}^{0,1+}, M(t\bar{t}), y(t\bar{t})]$ compared to NLO pred. with diff. α_s

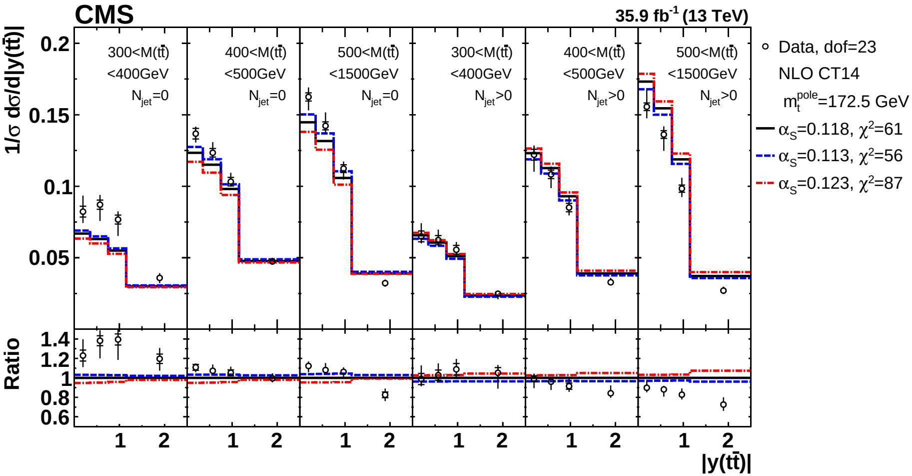

- α_s sensitivity comes from different N_{jet} bins
- further (indirect) sensitivity comes from $[M(t\bar{t}), y(t\bar{t})]$ via sensitivity to PDFs

Results: $[N_{\text{jet}}^{0,1+}, M(t\bar{t}), y(t\bar{t})]$ compared to NLO pred. with diff. m_t^{pole}

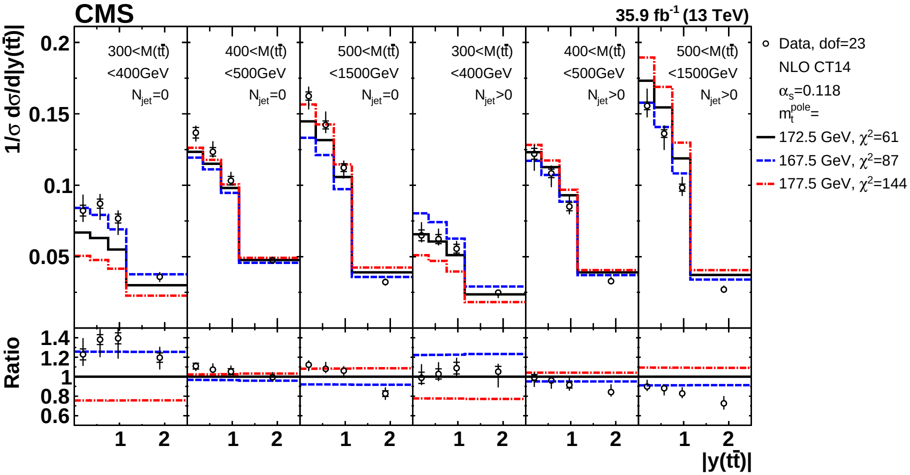

- m_t^{pole} sensitivity comes from $M(t\bar{t})$, mainly 1st bin
- this method differs from extracting m_t^{pole} from total $t\bar{t}$ x-section, and is similar to extracting m_t^{pole} from $t\bar{t}j$ diff. x-section [EPJ C73 (2013) 2438, CMS-PAS-TOP-13-006, JHEP 1510 (2015) 121]
- previous determination using this method: prelim. D0 results [FERMILAB-CONF-16-383-PPD]

Results: extraction of α_s from $[N_{\text{jet}}^{0,1+}, M(t\bar{t}), y(t\bar{t})]$

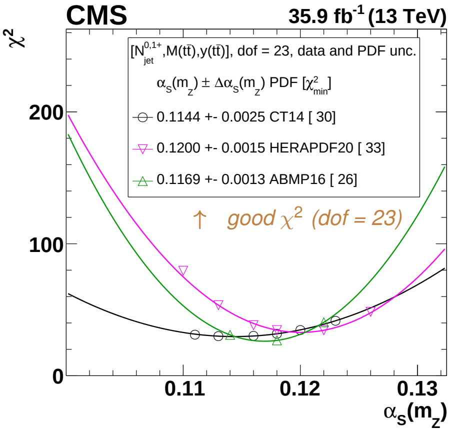

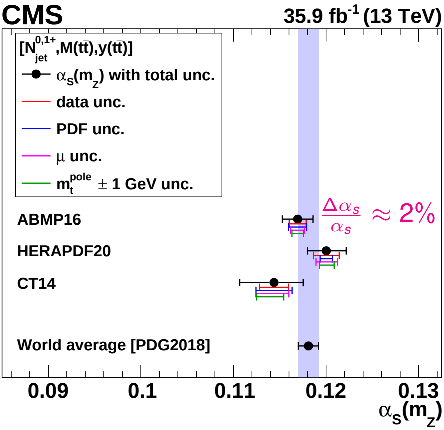

- precise determination of α_s is possible using these data
- significant dependence on PDF set observed (correlation between g and α_s)

Results: extraction of $m_t^{\rm pole}$ from $[N_{\rm jet}^{0,1+}, M(t\bar{t}), y(t\bar{t})]$

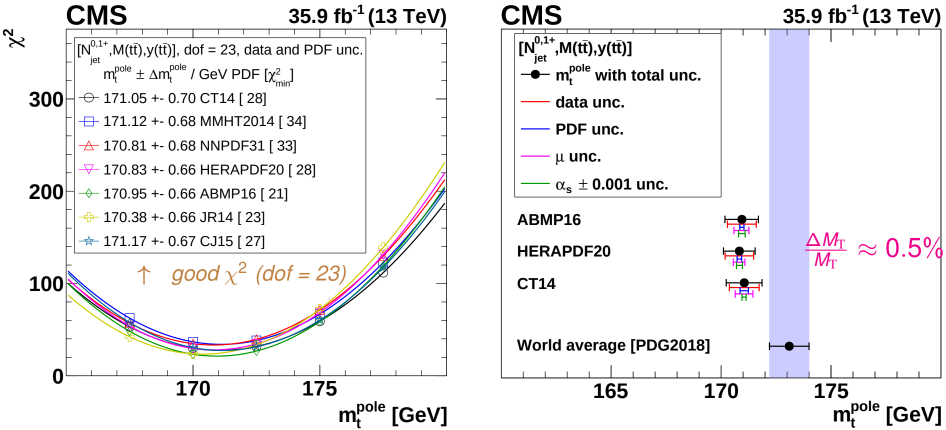

- precise determination of $m_t^{\rm pole}$: better than world average (2019)
- mild dependence on PDF set

Simultaneous PDF + α_s + m_t^{pole} fit: results

- followed standard approach: using HERA DIS data only, or HERA + $t\bar{t}$ data to demonstrate added value from $t\bar{t}$ on PDF and α_s determination
- using xFitter: open-source QCD fit framework [`xfitter.org`]

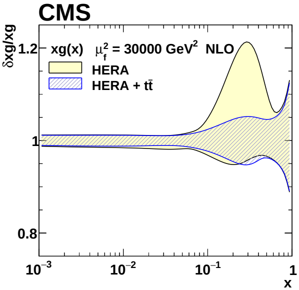

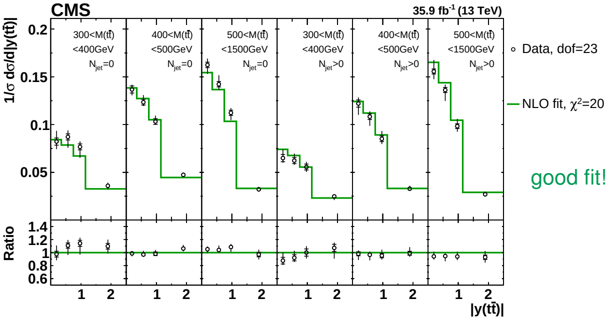

good fit!

$$\alpha_s(M_Z) = 0.1135 \pm 0.0016(\text{fit})^{+0.0002}_{-0.0004}(\text{mod})^{+0.0008}_{-0.0001}(\text{par})^{+0.0011}_{-0.0005}(\text{scale}) = 0.1135^{+0.0021}_{-0.0017}(\text{total})$$

$$m_t^{\text{pole}} = 170.5 \pm 0.7(\text{fit})^{+0.1}_{-0.1}(\text{mod})^{+0.0}_{-0.1}(\text{par})^{+0.3}_{-0.3}(\text{scale})\ \text{GeV} = 170.5 \pm 0.8(\text{total})\ \text{GeV}$$

$\rightarrow$ two SM parameters are simultaneously determined from these data to high precision with only weak correlation between them ($\rho = 0.3$) + constraints on PDFs

Simultaneous PDF + α_s + m_t^{pole} fit: correlation

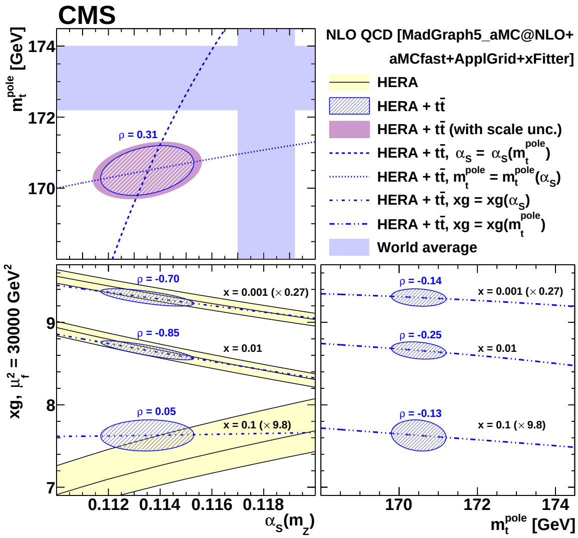

- For the first time studied correlations of m_t^{pole}, α_s and PDFs
- DESY and CERN CMS news highlighting this analysis

Pheno analysis of LHC $t\bar{t}$ data at NNLO [MATRIX+PineAPPL+xFitter] (Garzelli, Mazzitelli, Moch, Zenaiev, work in progress)

- NNLO calculations (q_T subtraction) for fully differential $t\bar{t}$ are ublicly available with MATRIX framework [Catani, Devoto, Grazzini, Kallweit, Mazzitelli Phys.Rev.D 99 (2019) 5, 051501; JHEP 07 (2019) 100]
  - fully differential NNLO calculations were also published in JHEP 04 (2017) 071 [Czakon, Heymes, Mitov], but no public code available
- Private version of MATRIX:
  - interfaced to PineAPPL [Carrazza at al., JHEP 12 (2020) 108] to produce PDF interpolation grids further used in xFitter `https://gitlab.com/fitters/xfitter`
    - reproduce NNLO calculations using any PDF and/or varied μ_r, μ_f in $\sim$ seconds
  - Improved technical performance for $t\bar{t}$ to achiev $\Delta\sigma_{t\bar{t}} = 0.5‰$
    - skip calculation of identical things (tailored for $t\bar{t}$)
    - adapted to DESY cluster + fixes related to memory and disk space usage etc.
- Runs with m_t^{pole} values 165–177.5 GeV with step of 2.5 GeV and $\Delta\sigma_{t\bar{t}} = 0.5‰$
  - $\approx 60000 \times 6 = 360000$ CPU hours (40 years)
  - for differential distributions, numerical uncertainties in bins are $\sim 0.5\%$
  - this is not negligible compared to data precision
    $\rightarrow$ 1% is included as theory uncertainty in χ^2 calculation
- Differential distributions obtained with fixed $r_{cut} = 0.0015$ (q_T subtraction)
  - verified vs. JHEP 07 (2019) 100: agreement within 1%
  - checked distributions with $r_{cut} = 0.0005$ (slower convergence) for $\sigma(t\bar{t})$: $< 1\%$
  - checked extrapolation to $r_{cut} = 0$ for $\sigma(t\bar{t})$: $< 1\%$
- $\mu_r = \mu_f = H_T/4$, $H_T = \sqrt{m_t^2 + p_T^2(t)} + \sqrt{m_{\bar{t}}^2 + p_T^2(\bar{t})}$, varied by factor 2 ($0.5 \leq \mu_r/\mu_f \leq 2$)

xFitter

Welcome to xFitter (former HERAFitter)

Proton parton distribution functions (PDFs) are essential for precision physics at the LHC and other hadron colliders. The determination of the PDFs is a complex endeavor involving several physics process. The main process is the lepton proton deep-inelastic scattering (DIS), with data collected by the HERA ep collider covering a large kinematic phase space needed to extract PDFs. Further processes (fixed target DIS, ppbar collisions etc.) provide additional constraining powers for flavour separation. In particular, the precise measurements obtained or to come from LHC will continue to improve the knowledge of the PDF.

The xFitter project is an open source QCD fit framework ready to extract PDFs and assess the impact of new data. The framework includes modules allowing for a various theoretical and methodological options, capable to fit a large number of relevant data sets from HERA, Tevatron and LHC. This framework is already used in many analyses at the LHC.

Downloads of xFitter software package

All the xFitter releases can be accessed HERE including **2.2.0 FutureFreeze** release
All the former (HERAFitter) releases can be accessed HERE.
Description: http://arxiv.org/abs/1410.4412

xFitter Meetings

xFitter Workshop at CERN 2-5 May 2023

- User's Meetings: meetings to enhance communication between users and developers (open access)
- Developer's Meeting: technical weekly meetings to ensure communication among developers (restricted access)
- Steering Group's Meeting (restricted access)

xFitter representation

- Snowmass contrubution
- List of results
- List of collected talks

Developers Info (restricted to developers)

- Internal Developments

Organisation

- **Release coordinator/Librarian** (revision of the release candidates): Sasha Glazov, Oleksandr Zenaiev
- **DESY IT Contact:** Yves Kemp

Getting help

See our help forum https://groups.google.com/forum/#!forum/xfitter-users
In case of questions or problems, please post a message there (requires a google account) or send it via email xfitter-users@googlegroups.com (no account required)

xFitter [xfitter.org] [gitlab.com/fitters/xfitter]

- **xFitter (HERAfitter before 2015) is a unique open-source QCD fit framework:**
  - extract PDFs and theory parameters
  - assess impact of new data
  - check consistency of experimental data
  - test different theoretical assumptions
  - . . . any exercise which involves data vs. theory
- It is widely used by LHC experiments and theorists ($>$ 100 publications)
- **Why is xFitter unique and so nice?**
  Because it is fully modular. E.g., hadron interactions are realized as
  - PDF parametrisation at starting scale: it is enough to type your favourite formulas
  - PDF decomposition: construct valence, sea and gluon, apply sum rules (automatic integration)
  - PDF evolution: interfaced various codes (QCDNUM, OPENQCDRAD, APFEL, LHAPDF); one can easily interace a new code
  - hard scattering ("reaction"): again, supports various options:
    - ★ various HQ schemes for ep DIS
    - ★ some "simple" calculations, e.g. LO DY
    - ★ interfaced external packages, e.g. HATHOR (NNLO HQ total $t\bar{t}$ and single t hadroproduction) and HVQMNR (NLO HQ differential hadroproduction)
    - ★ but main emphasis is put on interfaces to fast intepolation tables, such as fastNLO, ApplGrid, PineAppl: allows us to get recent higher-order calculations (e.g. MCFM, MATRIX etc.) "for free"
  - . . . and one can mix all these ingredients freely

- “A determination of $m_c(m_c)$ from HERA data using a matched heavy flavor scheme” [JHEP 1608 (2016) 050]
- “Probing the strange content of the proton with charm production in charged current at LHeC” [Eur. Phys. J. C 79, 864 (2019)]
- “PDF Profiling Using the Forward-Backward Asymmetry in Neutral Current Drell-Yan Production” [JHEP 2019, 176 (2019)]
- “Parton Distribution Functions of the Charged Pion Within The xFitter Framework” [Phys.Rev.D 102 (2020) 1, 014040]
- “Exploring SMEFT Couplings Using the Forward-Backward Asymmetry in Neutral Current Drell-Yan Production at the LHC” [work in progress, EPS2023 talk]

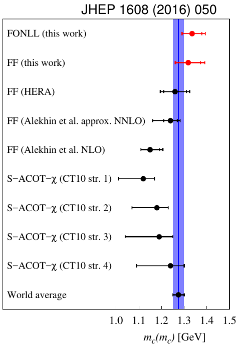

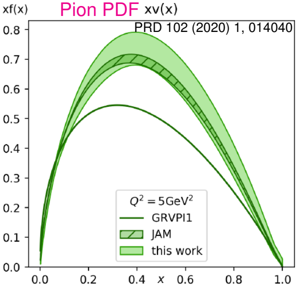

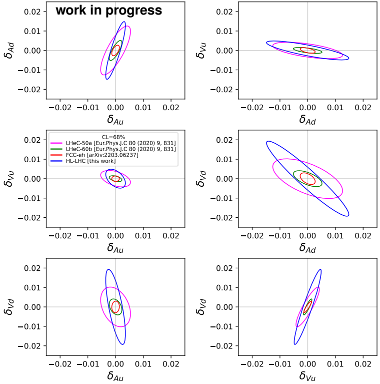

Data for pheno analysis (WIP)

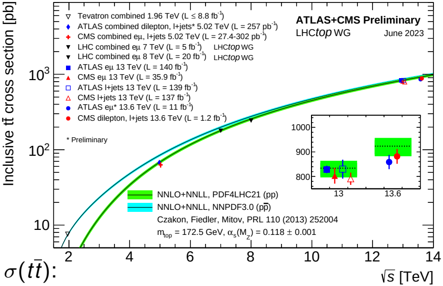

Selection of data:

- all measurements of total $t\bar{t}$ cross sections $\sigma(t\bar{t})$:
  - 10 data points, including recent combined CMS+ATLAS cross section at 7 and 8 TeV
- differential measurements $\frac{1}{\sigma(t\bar{t})}\frac{d\sigma(t\bar{t})}{dO}$ which satisfy following criteria:
  - as function of $M(t\bar{t})$ (if available, 2D $M(t\bar{t})$ and $y(t\bar{t})$)
  - at parton level (no cuts on p_T, y of leptons or jets)
  - normalized cross sections (to avoid unknown correlation with total $\sigma(t\bar{t})$)
  - bin-by-bin correlations are available

$$\sigma(t\bar{t})$$

Experiment	decay channel	dataset	luminosity	$\sqrt{s}$
ATLAS & CMS	combined	2011	5 fb^{-1}	7 TeV
ATLAS & CMS	combined	2012	20 fb^{-1}	8 TeV
ATLAS	dileptonic, semileptonic	2011	257 pb^{-1}	5.02 TeV
CMS	dileptonic	2011	302 pb^{-1}	5.02 TeV
ATLAS	dileptonic	2015-2018	140 fb^{-1}	13 TeV
ATLAS	semileptonic	2015-2018	139 fb^{-1}	13 TeV
CMS	dileptonic	2016	35.9 fb^{-1}	13 TeV
CMS	semileptonic	2016-2018	137 fb^{-1}	13 TeV
ATLAS	dileptonic	2022	11.3 fb^{-1}	13.6 TeV
CMS	dileptonic, semileptonic	2022	1.21 fb^{-1}	13.6 TeV

$$\frac{1}{\sigma(t\bar{t})}\frac{d\sigma(t\bar{t})}{dO}$$

Experiment	decay channel	dataset	luminosity	$\sqrt{s}$	observable(s)	n
CMS	semileptonic	2016–2018	137 fb^{-1}	13 TeV	$M(t\bar{t})$, $\lvert y(t\bar{t})\rvert$	34
CMS	dileptonic	2016	35.9 fb^{-1}	13 TeV	$M(t\bar{t})$, $\lvert y(t\bar{t})\rvert$	15
ATLAS	semileptonic	2015–2016	36 fb^{-1}	13 TeV	$M(t\bar{t})$, $\lvert y(t\bar{t})\rvert$	19
ATLAS	all-hadronic	2015–2016	36.1 fb^{-1}	13 TeV	$M(t\bar{t})$, $\lvert y(t\bar{t})\rvert$	10
CMS	dileptonic	2012	19.7 fb^{-1}	8 TeV	$M(t\bar{t})$, $\lvert y(t\bar{t})\rvert$	15
ATLAS	semileptonic	2012	20.3 fb^{-1}	8 TeV	$M(t\bar{t})$	6
ATLAS	dileptonic	2012	20.2 fb^{-1}	8 TeV	$M(t\bar{t})$	5
ATLAS	dileptonic	2011	4.6 fb^{-1}	7 TeV	$M(t\bar{t})$	4
ATLAS	semileptonic	2011	4.6 fb^{-1}	7 TeV	$M(t\bar{t})$	4

$\sigma(t\bar{t})$ vs NNLO predictions using different PDFs (WIP)

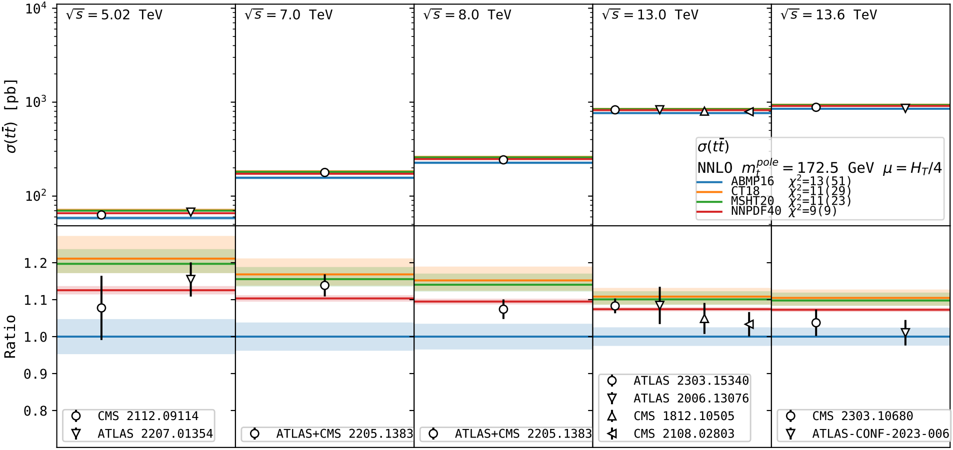

- Fixed $m_t^{\text{pole}} = 172.5$ GeV, $\mu_r = \mu_f = H_T/4$
- Reported χ^2 values with (and without) PDF uncertainties
- All PDF sets describe data reasonably well (depends on m_t^{pole}, α_S)
- Sensitivity to PDFs reduces with increasing $\sqrt{s}$ (lower x probed)

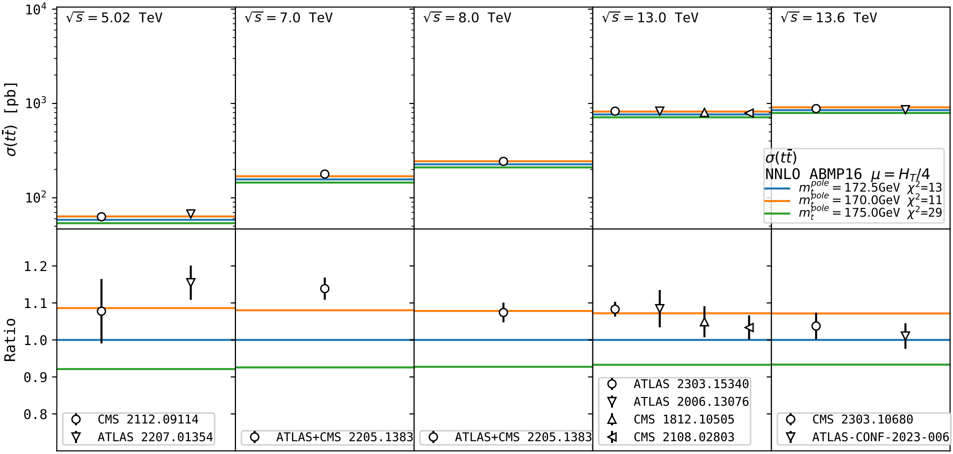

- ABMP16, fixed $\mu_r = \mu_f = H_T/4$
- Change of m_t^{pole} by 1 GeV $\rightarrow$ change of $\sigma(t\bar{t})$ by $\approx 3\%$
- Preferable $m_t^{\text{pole}} \sim 170$–$172.5$ GeV (depends on PDF and α_S)

$\sigma(t\bar{t})$ vs NNLO predictions with scale variations (WIP)

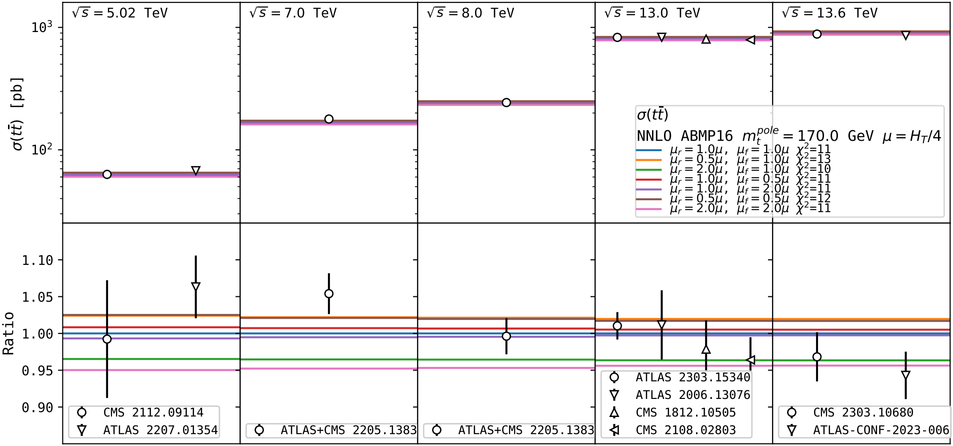

- ABMP16, fixed $m_t^{\text{pole}} = 172.5$ GeV
- Scale variations $^{+3\%}_{-5\%}$:
  - larger than data uncertainty (best data uncertainty $\pm 1.9\%$)
  - limit precision of m_t^{pole} extraction to 1 GeV
  - can be reduced by using e.g. $\overline{\text{MS}}$ mass $m_t(m_t)$ EPJ C74 (2014) 3167, JHEP04 (2021) 043

CMS 2108.02803 vs NNLO predictions using different PDFs (WIP)

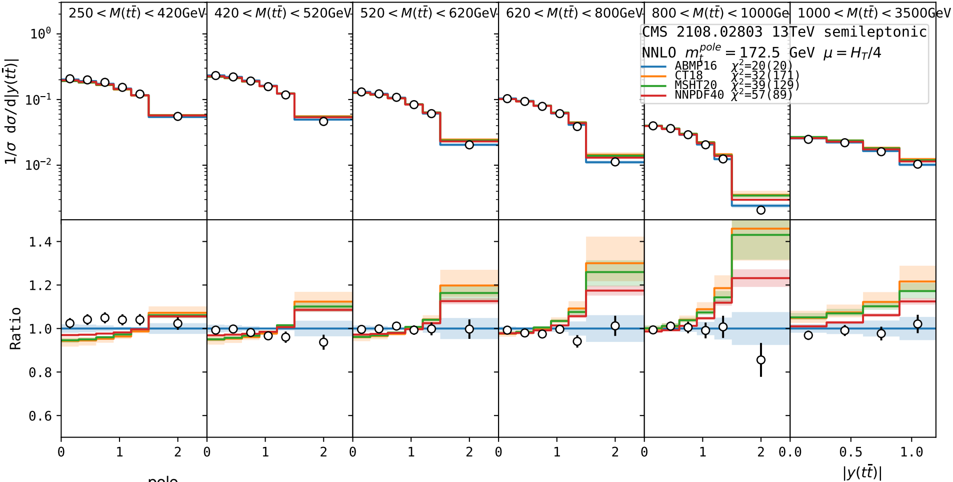

- Fixed $m_t^{\text{pole}} = 172.5$ GeV, $\mu_r = \mu_f = H_T/4$
- Reported χ^2 values with (and without) PDF uncertainties
- All PDF sets describe data reasonably well, with best description by ABMP16
  - CT18, MSHT20 and NNPDF40 show clear trend w.r.t data at high $y(t\bar{t})$ (large x)
- This is most precise currently available data set with finest bins

CMS 2108.02803 vs NNLO predictions using different PDFs (WIP)

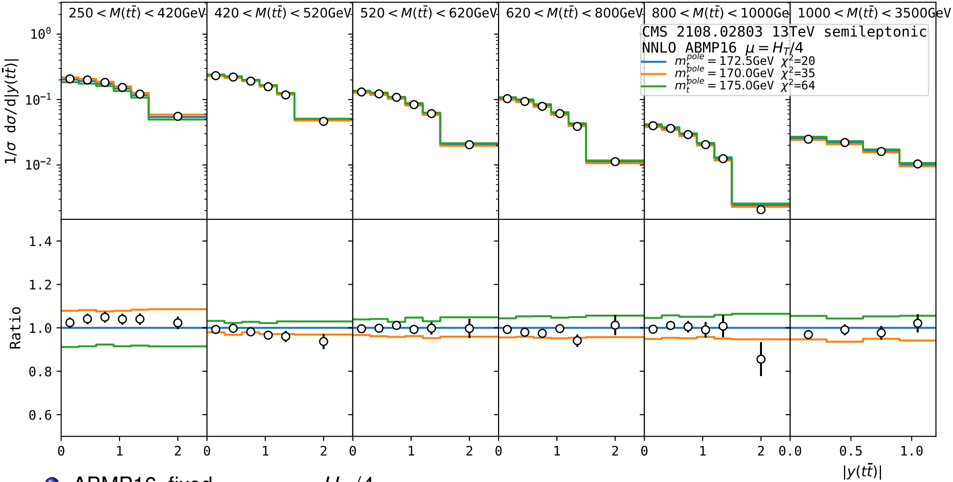

- ABMP16, fixed $\mu_r = \mu_f = H_T/4$
- Low $M(t\bar{t})$: strong dependence on m_t^{pole}via threshold effects
- High $M(t\bar{t})$: opposite dependence due to cross section normalization
- Preferable $m_t^{\text{pole}} \approx 172$ GeV

CMS 2108.02803 vs NNLO predictions using different PDFs (WIP)

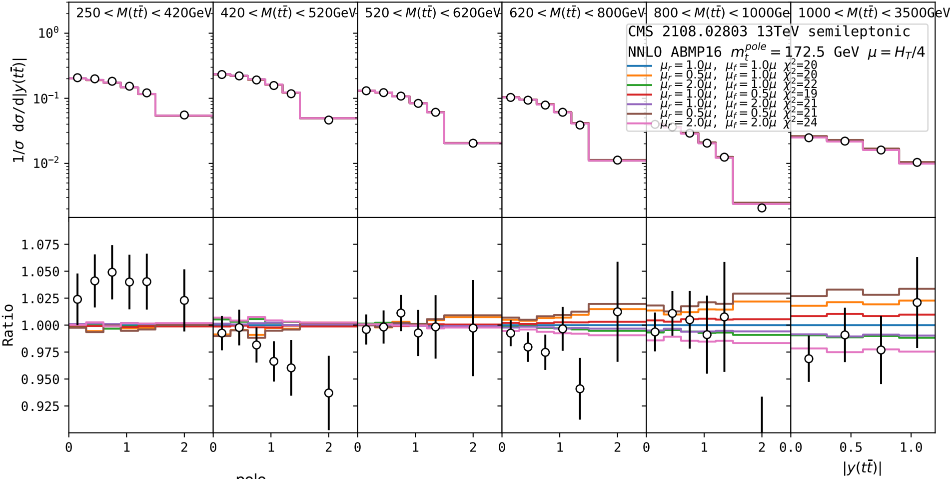

- ABMP16, fixed $m_t^{\text{pole}} = 172.5$ GeV
- Scale variations $< 1\%$ at low $M(t\bar{t})$ (largest cancellation), reach $\approx 4\%$ at high $M(t\bar{t})$

Extraction of m_t^{pole} (work in progress)

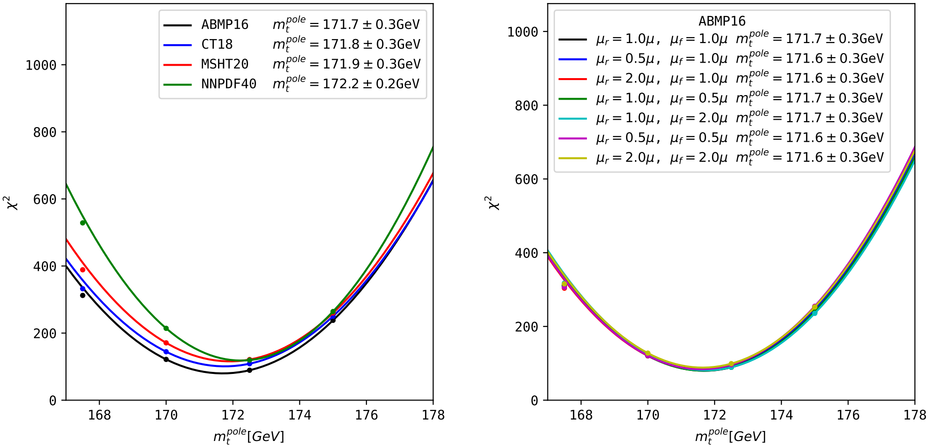

- Experimental, PDF and numerical theory uncertainties are included in χ^2
- Scale theory variations are not included in χ^2 but they are done explicitly (offset method) (typically amount to ±0.2 GeV)

Extraction of m_t^{pole}: differential Run 1, Run 2 (WIP)

Run 1 differential

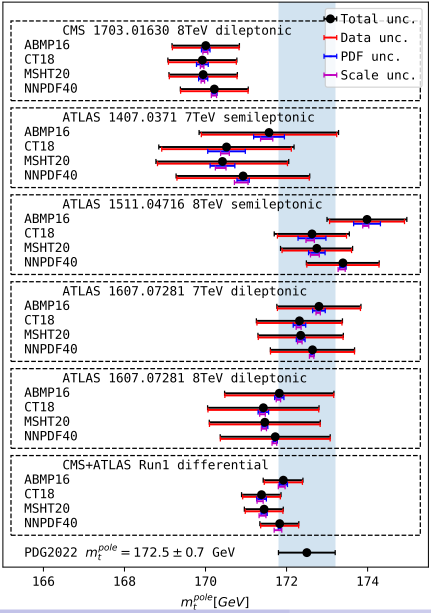

Run 2 differential

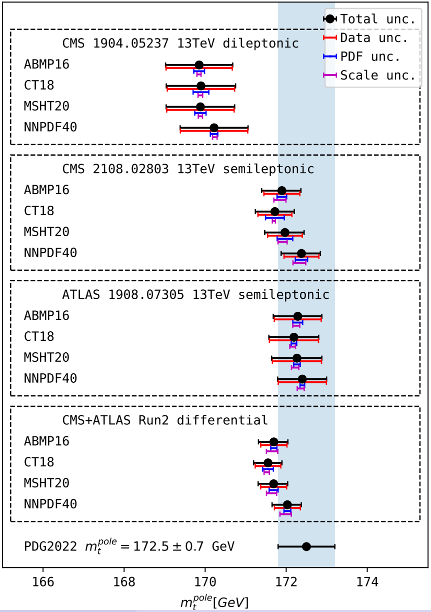

Extraction of m_t^{pole}: dilepton vs semileptonic, ATLAS vs CMS (WIP)

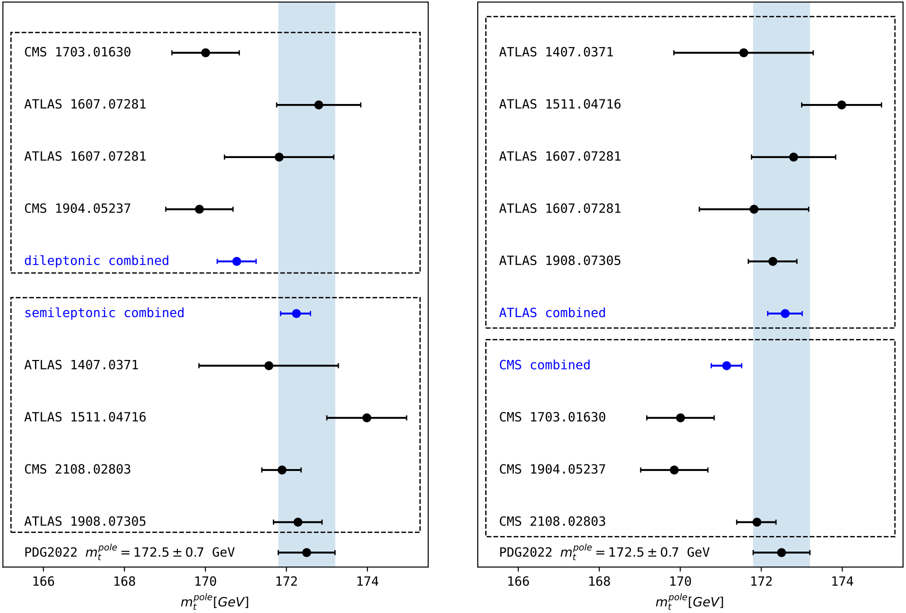

Extraction of m_t^{pole}: summary (work in progress)

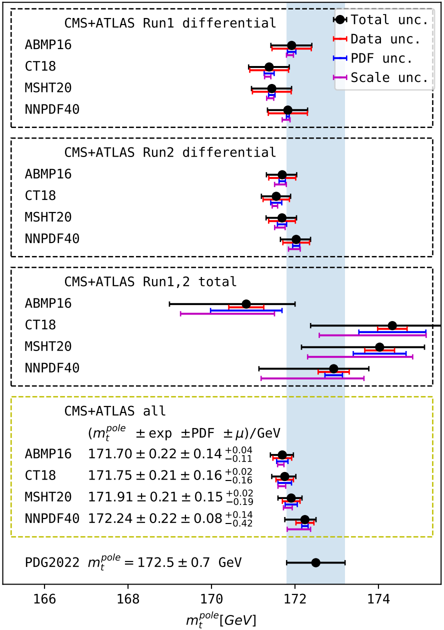

- Extracted m_t^{pole} values with precision ± 0.3 GeV are consistent with PDG value 172.5 ± 0.7 GeV
  - data uncertainty ~ 0.2 GeV
  - PDF uncertainty ~ 0.1 GeV
  - NNLO scale uncertainty ~ 0.2 GeV
- Significant dependence on PDFs (~ 0.5 GeV):
  - different m_t^{pole} used in different PDFs
  - PDFs, m_t^{pole}, α_s should be determined simultaneously
- For CMS 1904.05237, NNLO results are consistent with published results obtained at NLO
  - good convergence of perturbative series
- Larger sensitivity comes from differential data
  - 2D differential x-sections in $M(t\bar{t})$, $y(t\bar{t})$ constrain m_t^{pole}, PDFs and (indirectly) α_S
  - ideally, 3D cross section in $M(t\bar{t})$, $y(t\bar{t})$ and number of extra jets constrain α_S directly, but NNLO not yet available for $t\bar{t}$ +jets
- Possible effects from Coulomb and soft-gluon resummation near the $t\bar{t}$ production threshold are neglected: might be up to 1 GeV

[CMS Coll. EPJ C80 (2020) 658; Kiyo, Kuhn, Moch, Steinhauser, Uwer EPJ C60 (2009) 375; Mäkelä, Hoang, Lipka, Moch 2301.03546]

Summary

Many phenomenological applications of precision QCD with HQ:

- m_c, m_b extraction from HERA (ep) data + constraints on PDFs
  - high-precision final HERA data are in some tension with NLO and NNLO
- $c\bar{c}$ and $b\bar{b}$ production at LHC (pp): application for astrophysics
  - really need NNLO differential calculations (publicly available only for $t\bar{t}$)
- $t\bar{t}$ production at LHC (pp): precise determination of m_t^{pole} + constraints on PDFs and α_S
  - a lot of experimental data available: looking forward for ATLAS and CMS combination of differential $t\bar{t}$ measurements
  - staying tuned for Run-3 data

BACKUP

Atmospheric ν **are background for** *astrophysical* ν**:**

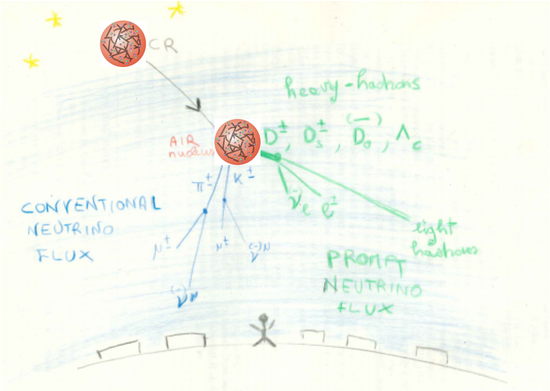

Production of atmospheric ν:

- cosmic rays (CR) + atmospheric nuclei
  → light and heavy hadrons → conventional and **prompt** ν fluxes
- spectra of conventional and **prompt** ν fluxes are different because of different hadroproduction cross sections and decay properties
- LHCb heavy-quark data improve predictions of **prompt** ν flux

PROSA PDFs and atmospheric ν fluxes [JHEP 1705 (2017) 004]

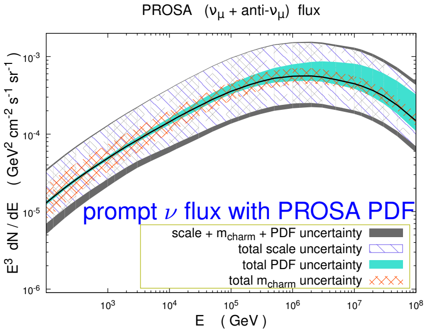

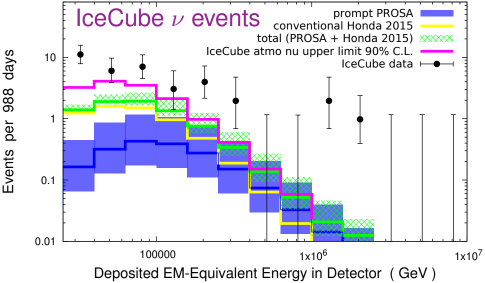

- Uncertainties for prompt ν flux are dominated by NLO scale uncertainties
- PDF uncertainties are under control owing to LHCb data in PROSA fit
- Predictions for the number of prompt, conventional and total expected atmospheric neutrino events for the IceCube 988-day HESE analysis, as compared to the IceCube lepton data
- IceCube upper limit lies well inside PROSA uncertainty band at high E_ν

$\rightarrow$ LHC data on hadroproduction and their interpretation are of crucial importance for astrophysical measurements

$\rightarrow$ astrophysical measurements provide complementary information about charm hadroproduction and proton structure

Parton distribution functions (PDFs)

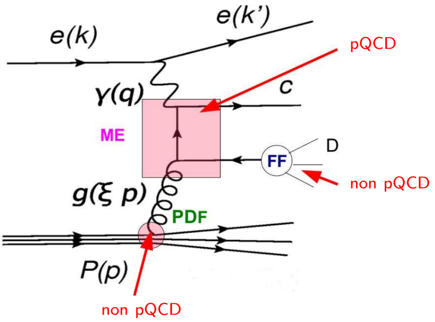

$$\sigma = \text{PDF} \otimes \text{ME} \otimes \text{FF}$$

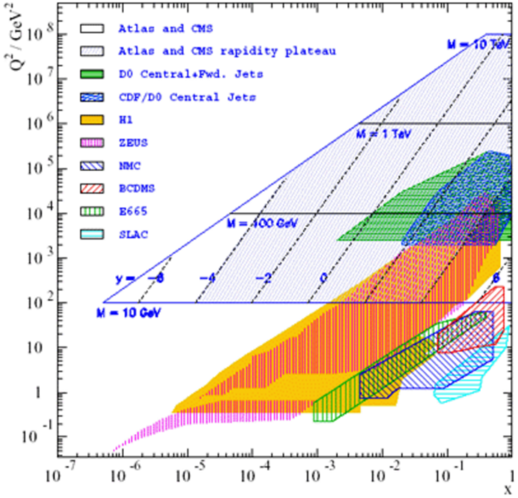

Measure σ, calculate ME $\Rightarrow$ determine PDF and/or FF

Parton distribution functions (PDFs)

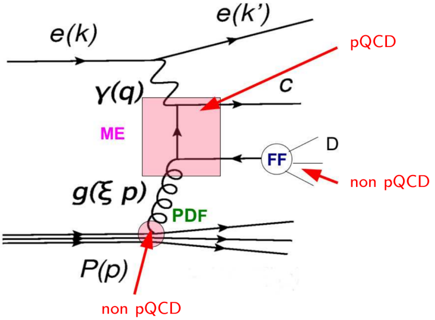

$$\sigma = \text{PDF} \otimes \text{ME} \otimes \text{FF}$$

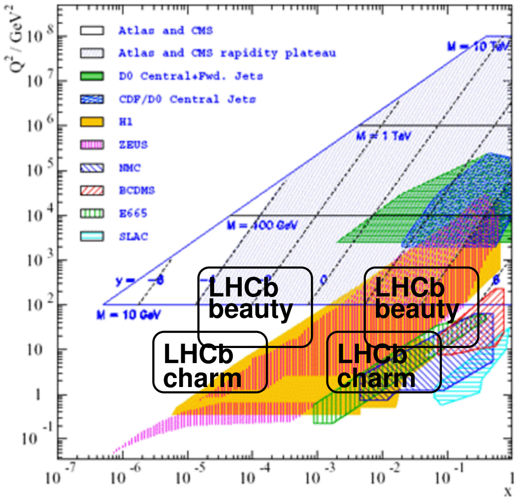

Measure σ, calculate ME $\Rightarrow$ determine PDF and/or FF

Kinematic distributions

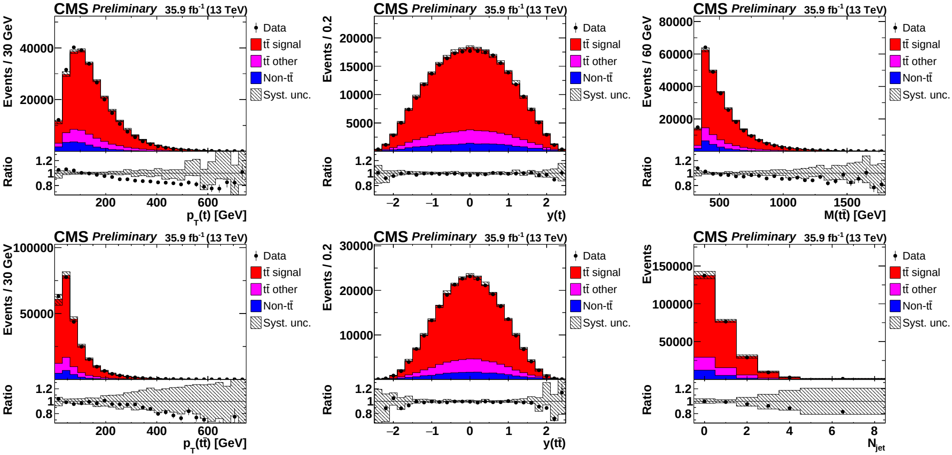

- $t\bar{t}$ signal MC: POWHEGV2 $+$ PYTHIA8
- Overall good description of data within uncertainties
- Central MC predictions for $p_T(t)$, $p_T(t\bar{t})$, $M(t\bar{t})$, N_{jet} are softer than data

Results: 2D x-sections $[y(t), p_T(t)]$

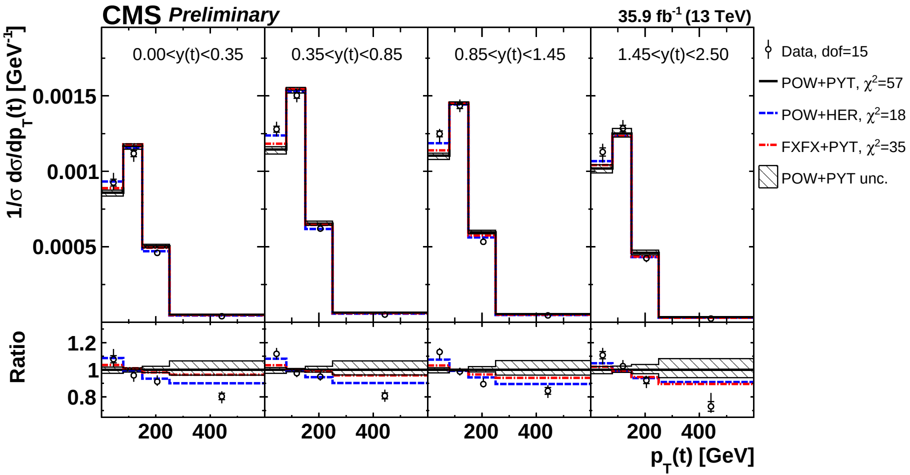

- ‘POW-PYT’ and ‘FXFX-PYT’ predict softer $p_T(t)$ in entire $y(t)$ range
- better description by ‘POW-HER’

Results: 2D cross sections $[M(t\bar{t}), p_T(t)]$

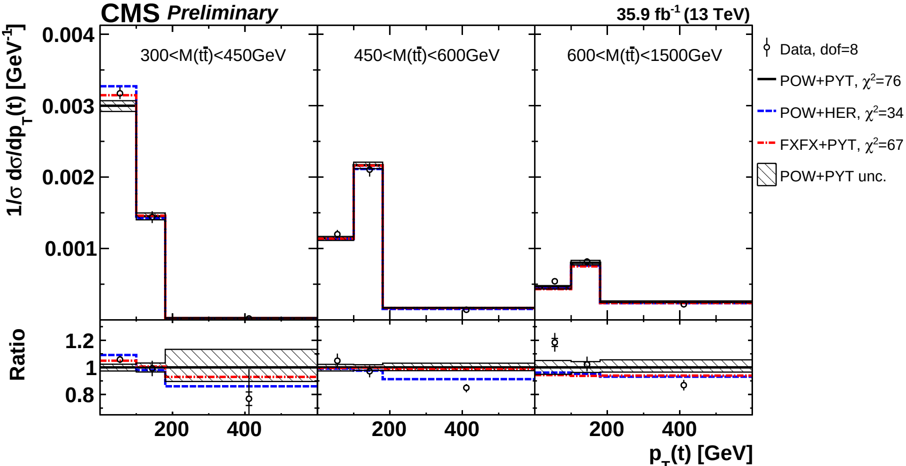

- bad description by all MC, strongest disagreement for 'POW-PYT'
- 'POW-HER' describes $p_T(t)$ in entire $y(t)$ range, but predicts too hard $p_T(t)$ at high $M(t\bar{t})$
  - can be observed only in 2D measurement

Results: 3D cross sections $[N_{\text{jet}}^{0,1,2+}, M(t\bar{t}), y(t\bar{t})]$

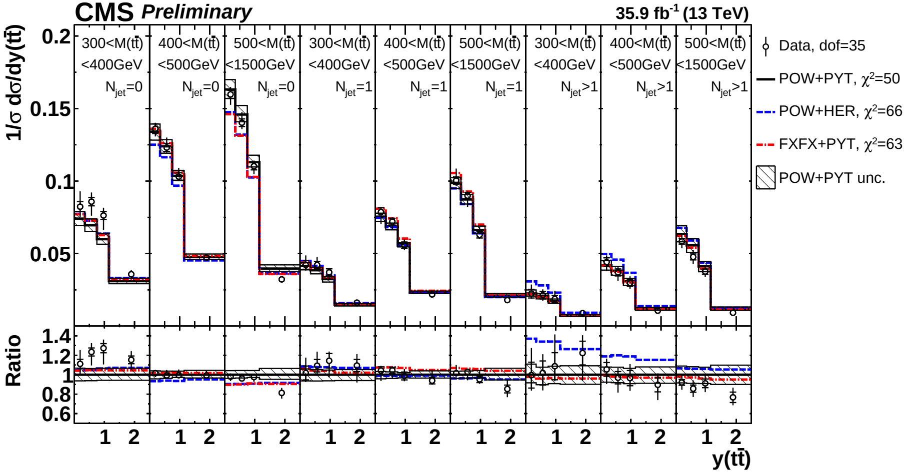

- 'POW-HER' predicts too high cross section at $N_{\text{jet}} > 1$
- 'FXFX-PYT' describes worse $M(t\bar{t})$ at $N_{\text{jet}} = 1$

Results: summary of comparison to MC models

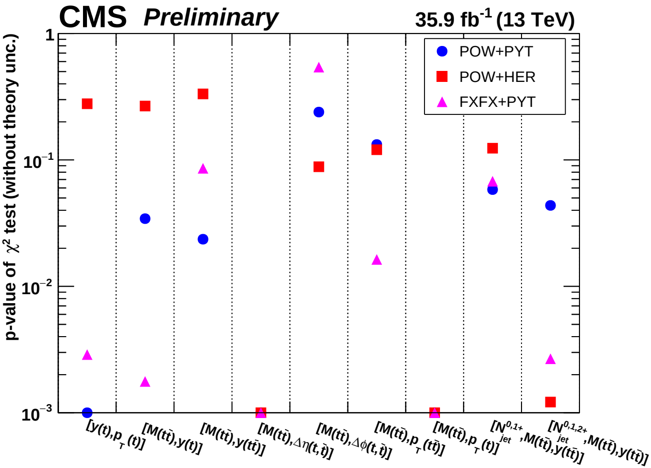

- none of central MC predictions is able to describe all distributions, in particular $[M(t\bar{t}), \Delta\eta(t,\bar{t})]$, $[M(t\bar{t}), p_T(t)]$
- overall, best description is provided by 'POW-PYT' and 'POW-HER':
  - 'POW-HER' describes better distributions probing $p_T(t)$
  - 'POW-PYT' describes better distributions probing $N_{\rm jet}$ and radiation

NLO calculations

- NLO predictions for inclusive $t\bar{t}$, $t\bar{t}$ + 1 jet and $t\bar{t}$ + 2 jets are computed and compared to data using MadGraph5_aMC@NLO + aMCfast + ApplGrid + xFitter:
  - $[N_{\rm jet}^{0,1+}, M(t\bar{t}), y(t\bar{t})]$ with 2 $N_{\rm jet}$ bins:
    - $\sigma^{\rm NLO}(N_{\rm jet} = 0) = \sigma^{\rm NLO}(t\bar{t}) - \sigma^{\rm NLO}(t\bar{t} + 1\text{jet})$
    - $\sigma^{\rm NLO}(N_{\rm jet} > 0) = \sigma^{\rm NLO}(t\bar{t} + 1\text{jet})$
  - $[N_{\rm jet}^{0,1,2+}, M(t\bar{t}), y(t\bar{t})]$ with 3 $N_{\rm jet}$ bins:
    - $\sigma^{\rm NLO}(N_{\rm jet} = 0) = \sigma^{\rm NLO}(t\bar{t}) - \sigma^{\rm NLO}(t\bar{t} + 1\text{jet})$
    - $\sigma^{\rm NLO}(N_{\rm jet} = 1) = \sigma^{\rm NLO}(t\bar{t} + 1\text{jet}) - \sigma^{\rm NLO}(t\bar{t} + 2\text{jets})$
    - $\sigma^{\rm NLO}(N_{\rm jet} > 1) = \sigma^{\rm NLO}(t\bar{t} + 2\text{jets})$
- $\mu_{\rm r} = \mu_{\rm f} = H'/2$, $H' = \sum_i m_{T,i}$ where the sum runs over all final-state partons (t, $\bar{t}$ and up to three light partons in the $t\bar{t} + 2$ jets calculations) and $m_T = \sqrt{m^2 + p_T^2}$. Uncertainties:
  - $\mu_{\rm r}, \mu_{\rm f}$ are varied by factor 2 (6 variations in total)
  - alternative functional form $\mu_{\rm r} = \mu_{\rm f} = H/2$, $H = \sum_i m_{T,i}$ with the sum runs over t and $\bar{t}$
- $m_t^{\rm pole} = 172.5 \pm 1$ GeV (sometimes ± 5 GeV for presentation purposes)
- PDFs and α_s from several groups via LHAPDF, $\alpha_s \pm 0.001$ for uncertainties (sometimes ± 0.005 for presentation purposes)
- multiplied with non-perturbative corrections ($< 5\%$) from parton to particle jet level (BACKUP)

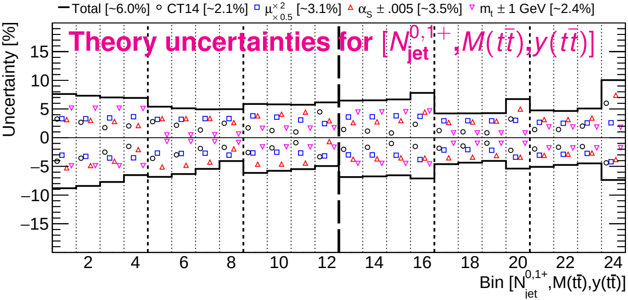

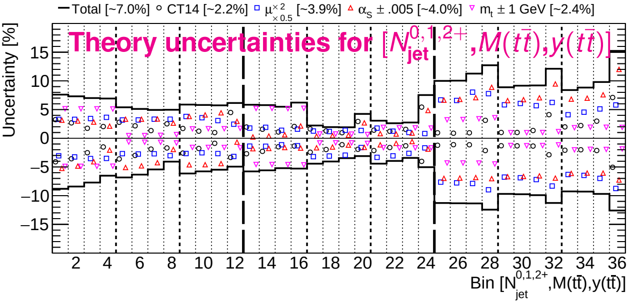

- Bins are grouped for $y(t\bar{t})$, $M(t\bar{t})$ and N_{jet} (separated by different vertical lines)
- NLO scale uncertainties are comparable to PDF, α_s and M_{T} uncertainties

  $\rightarrow$ data can constrain PDF, α_s and M_{T}
- Scale uncertainties are considerably smaller for $[N_{\mathrm{jet}}^{0,1+}, M(t\bar{t}), y(t\bar{t})]$

  $\rightarrow$ $[N_{\mathrm{jet}}^{0,1,2+}, M(t\bar{t}), y(t\bar{t})]$ is used for cross check only

Data interpretation consists of two parts:

(1) comparison theory vs data using external PDF sets:

- extracting α_s keeping m_t^{pole} fixed
- extracting m_t^{pole} keeping α_s fixed

(2) simultaneous fit of PDFs, α_s and m_t^{pole} using $t\bar{t}$ and HERA DIS:

$\rightarrow$ this presents fully consistent extraction of α_s, m_t^{pole} and PDFs

$\rightarrow$ important as exercise to understand new $t\bar{t}$ data, providing baseline for future global fits

Results: $[N_{\text{jet}}^{0,1+}, M(t\bar{t}), y(t\bar{t})]$ compared to NLO pred. with diff. PDFs

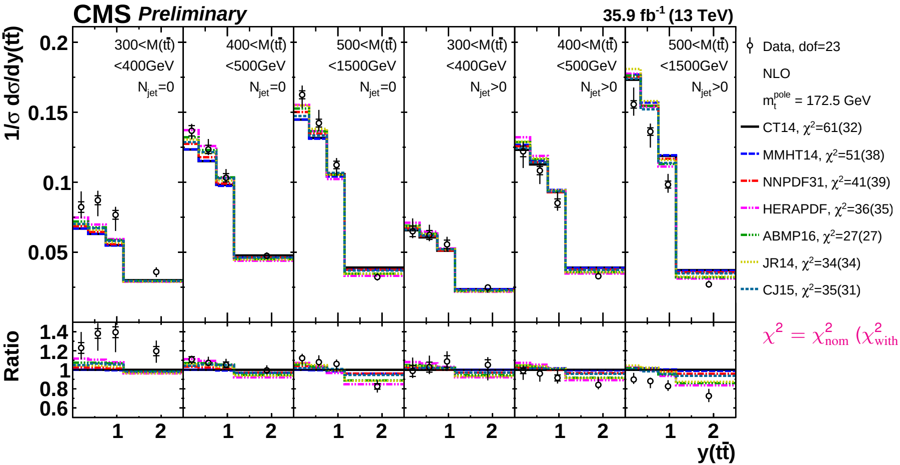

$\chi^2 = \chi^2_{\text{nom}}\ (\chi^2_{\text{with PDF unc.}})$

- description depends on PDFs $\rightarrow$ data are sensitive to PDFs
- all modern PDF sets considered
    - best description given by ABMP16

Results: $[N_{\text{jet}}^{0,1+}, M(t\bar{t}), y(t\bar{t})]$ compared to NLO pred. with diff. α_s

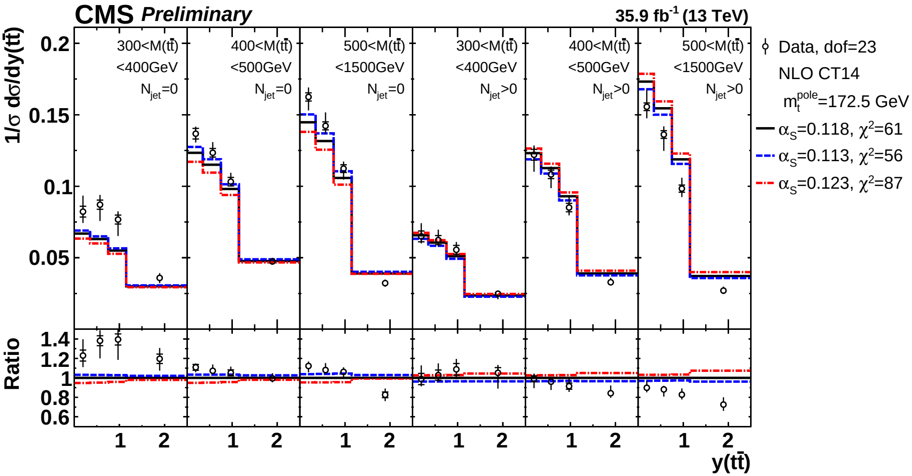

- α_s sensitivity comes from different N_{jet} bins
- further (indirect) sensitivity comes from $[M(t\bar{t}), y(t\bar{t})]$ via sensitivity to PDFs

Results: $[N_{\mathrm{jet}}^{0,1+}, M(t\bar{t}), y(t\bar{t})]$ compared to NLO pred. with diff. m_t^{pole}

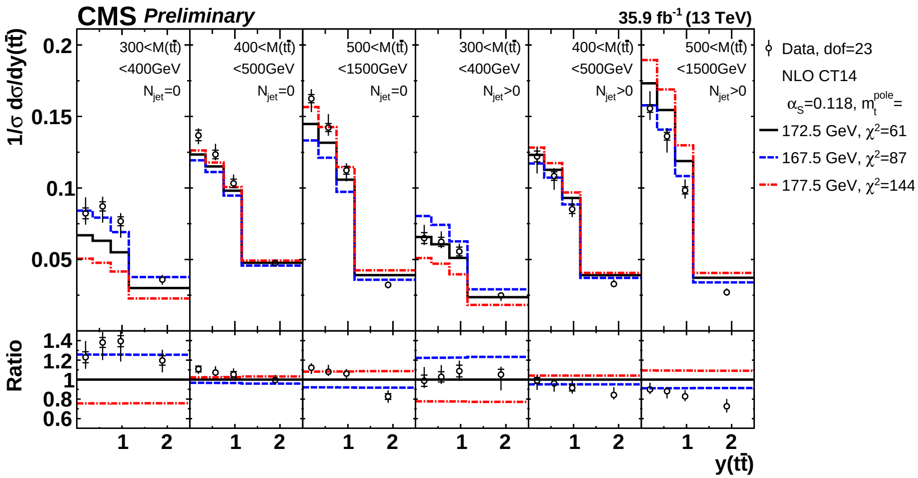

- M_{T} sensitivity comes from $M(t\bar{t})$, mainly 1st bin
- this method differs from extracting m_t^{pole} from total $t\bar{t}$ x-section, and is similar to extracting m_t^{pole} from $t\bar{t}j$ diff. x-section [EPJ C73 (2013) 2438, CMS-PAS-TOP-13-006, JHEP 1510 (2015) 121]
- previous determination using this method: prelim. D0 results [FERMILAB-CONF-16-383-PPD]

Cross checks of α_s and m_t^{pole} extraction (all results in backup):

- using $[N_{\text{jet}}^{0,1,2+}, M(t\bar{t}), y(t\bar{t})]$
- using single-differential N_{jet}, $M(t\bar{t})$ or $y(t\bar{t})$ cross sections
- using $[p_T(t\bar{t}), M(t\bar{t}), y(t\bar{t})]$ cross sections with 2 $p_T(t\bar{t})$ bins
- using unnormalised cross sections

→ consistent results obtained in all cross checks

→ in this analysis, observables ($\frac{1}{\sigma}\frac{d\sigma}{d\ldots}$) have been chosen to have **maximum sensitivity to QCD paramaters and minimum experimental and scale uncertainties**

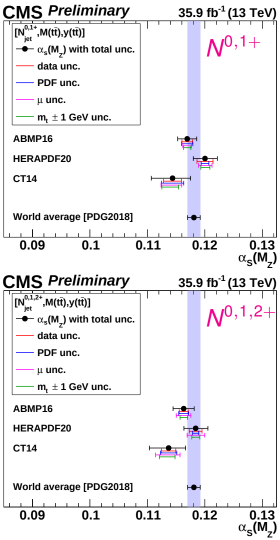

PDFs (α_s in HERA-only fit set to $\alpha_s = 0.1135 \pm 0.0016$)

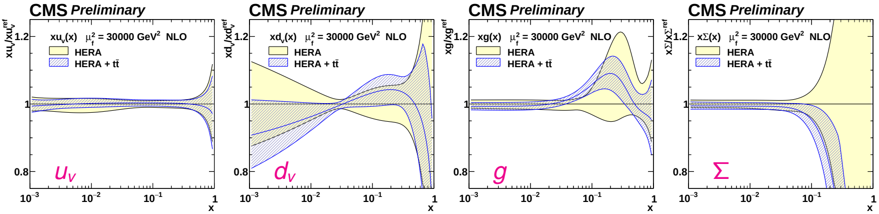

Relative PDF uncertainties

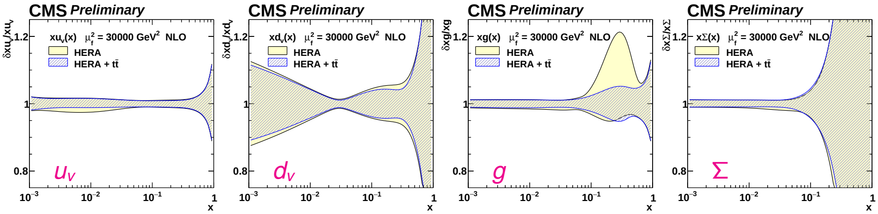

→ reduced g uncertainty at high x

→ smaller impact on other distributions

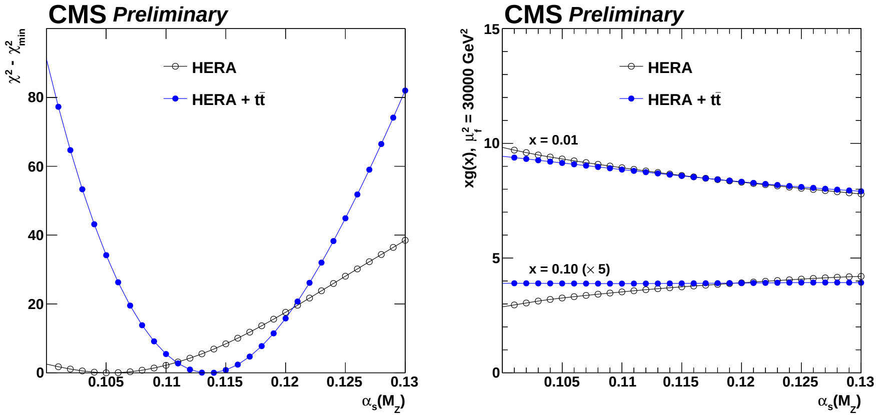

Adding $t\bar{t}$ data:

- constrain α_s (left)
- reduce correlation between α_s and gluon (g) (right)
  - weak correlation (α_s,M_{T}) $\rightarrow$ weak correlation (g,M_{T})

TOP-18-004 checks

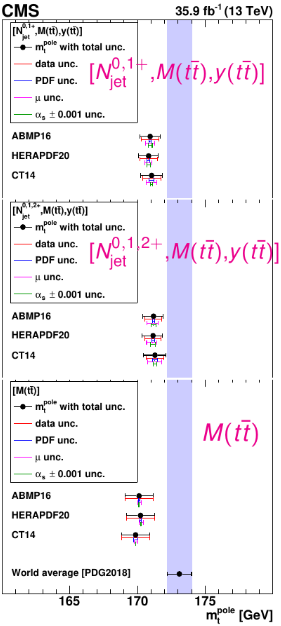

DESY 2018 summer school, L. Materne, bachelor thesis "Differential Top-Pair Production Cross Section with the CMS Detector - Optimization of Measurement Information", Karlsruher Institut für Technologie (KIT), Bachelorarbeit, 2018 [ETP-Bachelor-KA/2018-11]

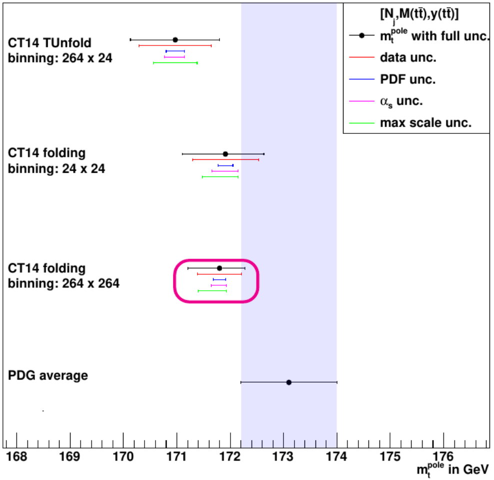

m_t dependence of measured cross sections

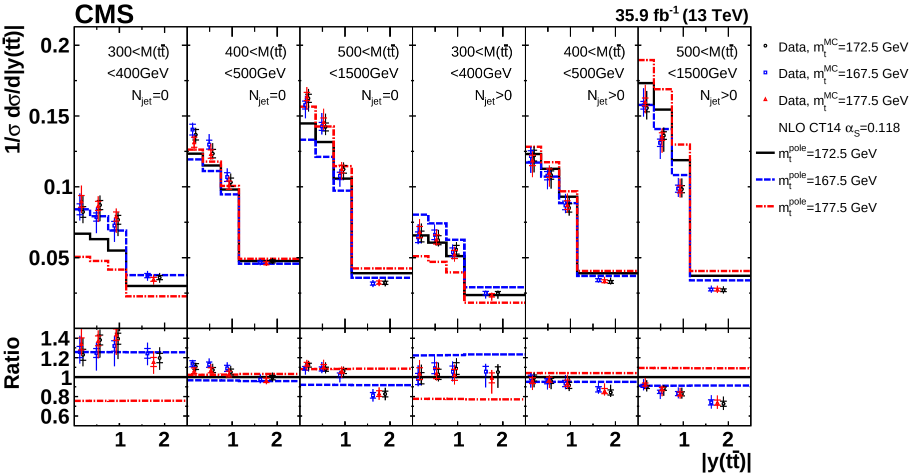

- Few studies of beauty baryon decays to final states involving a single open-charm meson

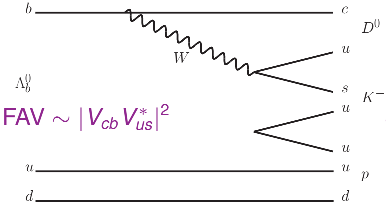

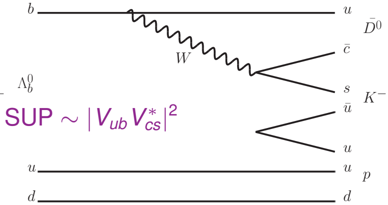

- We studied singly- and doubly-Cabibbo-suppressed $\Lambda_b^0 \to [K^+\pi^-]_D pK^-$ decays:
  - $\Lambda_b^0 \to [K^-\pi^+]_D pK^- \sim |V_{cb}V_{us}^*|^2$ is relatively favoured (FAV)
  - $\Lambda_b^0 \to [K^+\pi^-]_D pK^- \sim |V_{ub}V_{cs}^*|^2$ is relatively suppressed (SUP): *not yet observed*
    (FAV and SUP are defined by the relative charges of K from D and K from Λ_b^0)
  - $R_{\text{pred}} = \left|\frac{V_{cb}V_{us}^*}{V_{ub}V_{cs}^*}\right|^2 \approx 7.4$
- The suppressed decay receives contributions from $\Lambda_b^0 \to [K^+\pi^-]_{D^0} pK^-$ and $\Lambda_b^0 \to [K^+\pi^-]_{\bar{D}^0} pK^-$, leading to interference between them, CP violation and γ sensitivity [ADS method, PRL 78 (1997) 3257, PRD 63 (2001) 036005]
- Goals of this analysis:
  - observation of suppressed decay $\Lambda_b^0 \to [K^+\pi^-]_D pK^-$
  - measurement of ratio R and asymmetry A in full phase space and restricted region $M^2(pK^-) < 5$ GeV^2 with enhanced γ sensitivity

Observation of suppressed $\Lambda_b^0 \to [K^+\pi^-]_D pK^-$ decay and measurement of its CP asymmetry [LHCb Coll., Phys. Rev. D104 (2021) 112008]

- BDT selection (TMVA), simultaneous unbinned ML fit (RooFit) of favoured and suppressed decays (taking into account several partially reconstructed decays)

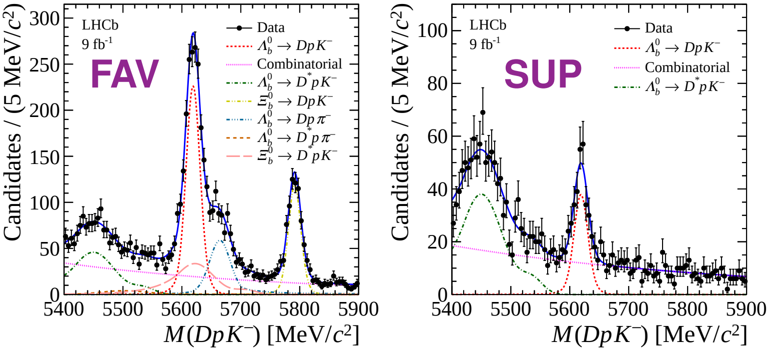

- **first observation** of suppressed decay $\Lambda_b^0 \to (K^+\pi^-)_D pK^-$ (241 ± 22 events)
- $R = \frac{\mathcal{B}(\Lambda_b^0 \to [K^-\pi^+]_D pK^-)}{\mathcal{B}(\Lambda_b^0 \to [K^+\pi^-]_D pK^-)} = 7.14 \pm 0.79(\text{stat.})^{+0.43}_{-0.33}(\text{syst.})$ [consistent with $R_{\text{pred}} \approx 7.4$]
- $A = \frac{N_{\text{SUP}}(\Lambda_b^0) - N_{\text{SUP}}(\overline{\Lambda_b^0})}{N_{\text{SUP}}(\Lambda_b^0) + N_{\text{SUP}}(\overline{\Lambda_b^0})} = 0.119 \pm 0.088(\text{stat.})^{+0.024}_{-0.026}(\text{syst.})$ [consistent with 0, but larger data sample is expected to be collected soon, and this mode will contribute to γ determination]

Introduction

- Few studies of beauty baryon decays to final states involving a single open-charm meson exist

$\Lambda_b^0 \to [K^-\pi^+]_D p\pi^-$

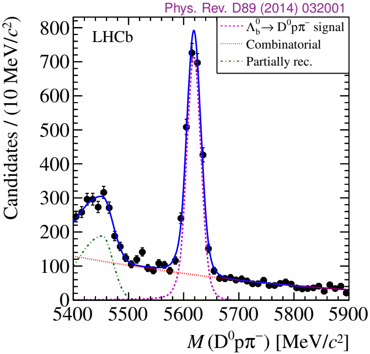

$\Lambda_b^0 \to [K^-\pi^+]_D pK^-$ [1st observation]

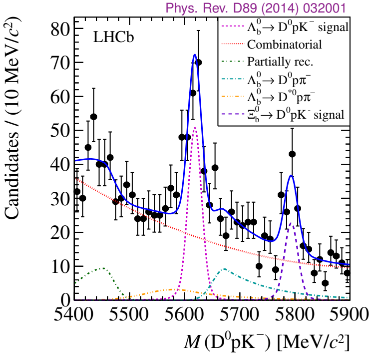

- In this analysis we study even further suppressed $\Lambda_b^0 \to [K^+\pi^-]_D pK^-$ decay:
  - $\Lambda_b^0 \to [K^-\pi^+]_D pK^- \sim |V_{cb}V_{us}^*|^2$ is relatively favoured (FAV)
  - $\Lambda_b^0 \to [K^+\pi^-]_D pK^- \sim |V_{ub}V_{cs}^*|^2$ is relatively suppressed (SUP): *not yet observed*

  (FAV and SUP are defined by the relative charges of K from D and K from Λ_b^0)

Analysis goals and strategy

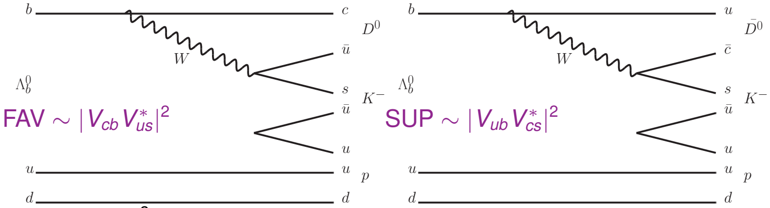

- $R_{\text{pred}} = \left| \frac{V_{cb}V_{us}^*}{V_{ub}V_{cs}^*} \right|^2 \approx 7.4$
- The suppressed decay receives contributions from $\Lambda_b^0 \to [K^+\pi^-]_{D^0}pK^-$ and $\Lambda_b^0 \to [K^+\pi^-]_{\bar{D}^0}pK^-$, leading to interference between them, CP violation and γ sensitivity [ADS method, PRL 78 (1997) 3257, PRD 63 (2001) 036005]
- Goals of this analysis:
  - observation of suppressed decay $\Lambda_b^0 \to [K^+\pi^-]_D pK^-$
  - measurement of ratio $R = \frac{\mathcal{B}(\Lambda_b^0 \to [K^-\pi^+]_D pK^-)}{\mathcal{B}(\Lambda_b^0 \to [K^+\pi^-]_D pK^-)}$
  - measurement of asymmetry $A = \frac{\mathcal{B}(\Lambda_b^0 \to [K^+\pi^-]_D pK^-) - \mathcal{B}(\bar{\Lambda}_b^0 \to [K^-\pi^+]_D \bar{p}K^+)}{\mathcal{B}(\Lambda_b^0 \to [K^+\pi^-]_D pK^-) + \mathcal{B}(\bar{\Lambda}_b^0 \to [K^-\pi^+]_D \bar{p}K^+)}$
  - measure R and A in restricted region $M^2(pK^-) < 5$ GeV^2 with enhanced γ sensitivity
- Similar to previous analysis:
  - study of $\Lambda_b^0 \to Dph$, $\Lambda_b^0 \to \Lambda_c h$ [Phys. Rev. D89 (2014) 032001, LHCb-ANA-2012-096]
  - AmAn $\Lambda_b^0 \to Dp\pi^-$ [JHEP 1705 (2017) 030, LHCb-ANA-2015-072]
- All analysis ingredients (selection, fits etc.) developed without using suppressed data events

BDT selection (TMVA)

- Using ROOT TMVA BDT (adaptive boosting with default settings), 16 variables (distributions in backup):

Variable	Λ_b^0	D^0	π_D	K_D	p	K
χ^2 of DTF	×					
χ^2 of vertex	×	×				
p_T asymmetry in cone of 1.5	×					
$c\tau$ significance	×	×				
IP χ^2	×	×				
$\Delta LL_{K\pi}$			×	×		×
probNN					×	
p_T	×	×	×	×		

- checked also MLP method: similar results
- checked separate training in Run1 and Run2: similar results

- Training samples:
  - signal: MC $\Lambda_b^0 \to (K^-\pi^+)_{D^0} pK^-$
  - background: DATA Λ_b^0 mass sidebands $5300 < M < 5400 \,||\, 5900 < M < 6000$ MeV
- Choosing working point (cut on BDT classifier):
  - optimise significance ($S/\sqrt{S+B}$) for suppressed decay, assuming $R = \mathrm{FAV}/\mathrm{SUP} = 7.4$
  - $\rightarrow$ expecting suppressed signal $\sim 200 \pm 20$ ($S/\sqrt{S+B} \sim 10$, or 10% stat. unc.)

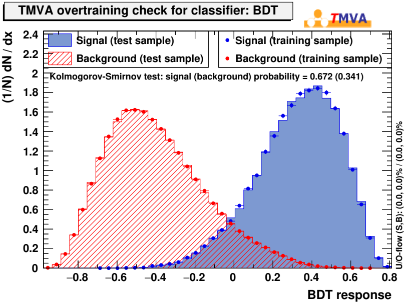

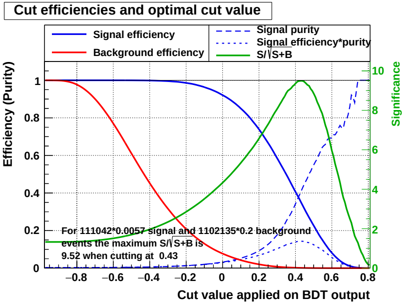

Final selection

Further cuts applied to suppress charmless background $\Lambda_b^0 \to ph^- h^+ h^-$:

- significance of D decay time > 2.5
- $|M([K\pi]_D) - m(D)| < 15$ MeV

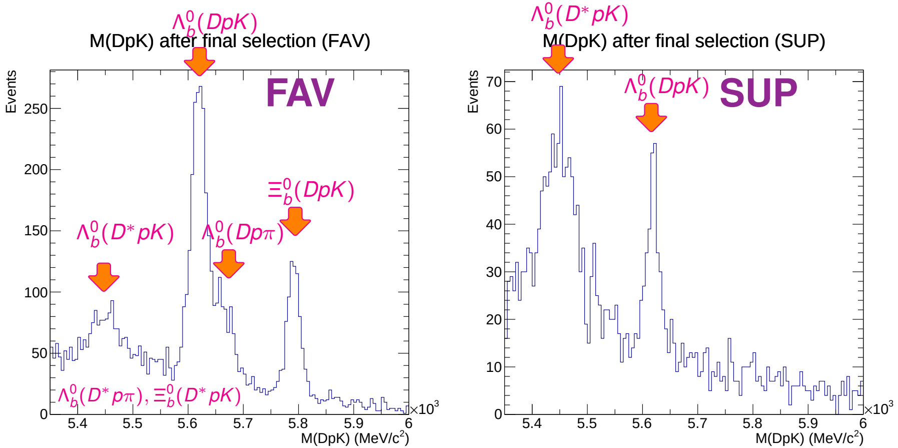

No $\Xi_b^0 \to DpK(\pi)$, $\Lambda_b^0 \to D^{(*)}p\pi$ expected in the suppressed decay (totally negligible)

Dalitz plot: favoured decay

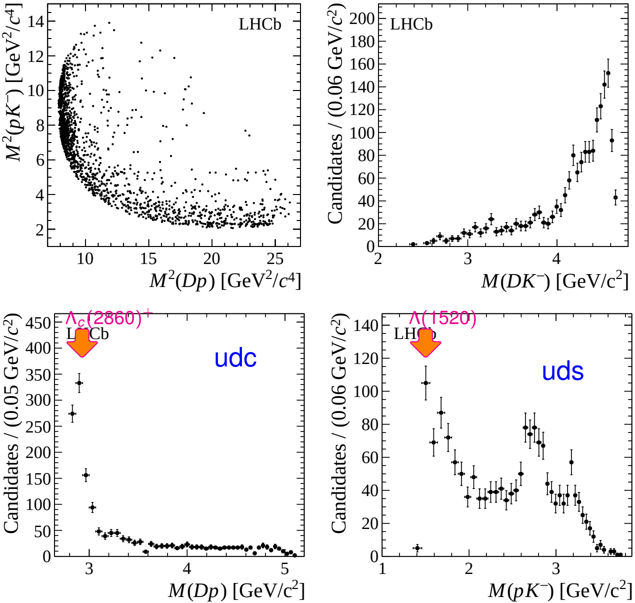

Dalitz plot: suppressed decay

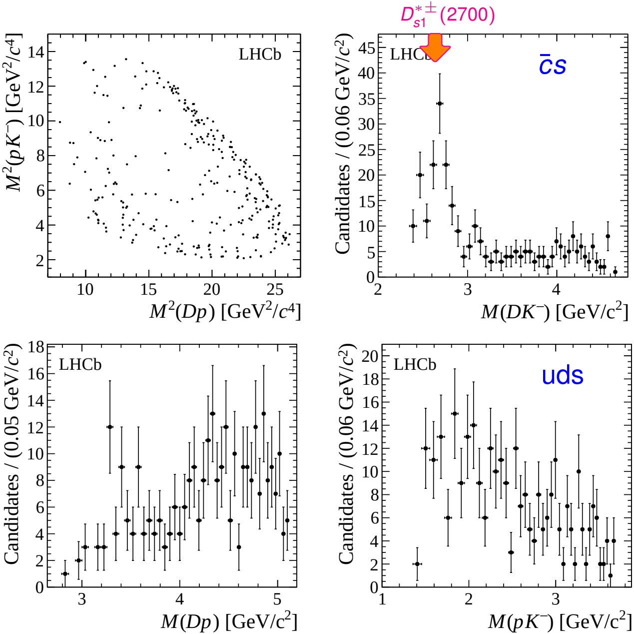

Efficiency correction and measurement of R and A in full phase space

- Efficiency includes reconstruction, selection and kinematic acceptance
- Relative efficiency is determined across the Dalitz plot variables (with D^0 and Λ_b^0 masses constrained), assuming unpolarised Λ_b^0, and parametrised using kernel-based PDF (Meerkat)
  - overall, relative efficiency is flat, varying within 0.7–1.2
- s-weights from invariant mass fits and efficiency corrections are
  - $R = \frac{\mathcal{B}(\Lambda_b^0 \to [K^-\pi^+]_D pK^-)}{\mathcal{B}(\Lambda_b^0 \to [K^+\pi^-]_D pK^-)} = 7.14 \pm 0.79(\text{stat.})^{+0.43}_{-0.33}(\text{syst.})$
  - $A = \frac{N_{\text{SUP}}(\Lambda_b^0) - N_{\text{SUP}}(\overline{\Lambda_b^0})}{N_{\text{SUP}}(\Lambda_b^0) + N_{\text{SUP}}(\overline{\Lambda_b^0})} = 0.119 \pm 0.088(\text{stat.})^{+0.024}_{-0.026}(\text{syst.})$

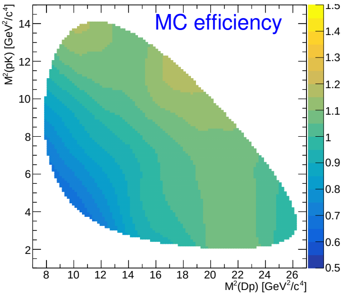

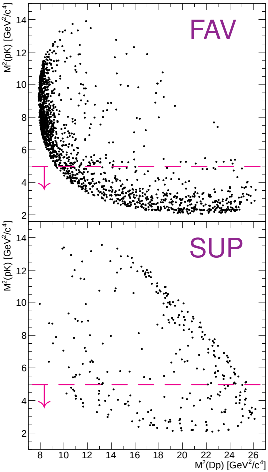

Measurement of R and A in restricted phase space $M^2(pK) < 5$ GeV^2

- sensitivity to CP-violation requires interference between amplitudes involving intermediate D^0 and $\bar{D}^0$ mesons in a region of the Dalitz plot
- $M^2(pK) < 5$ GeV^2 is chosen which contains the observed $\Lambda(1520)$ contribution, and balances sensitivity and statistics
- the same measurement procedure is used, except
  - BDT is trained in the $M^2(pK) < 5$ GeV^2 region
  - another parametrised PDF (bifurcated Gaus + CB) for $\Lambda_b^0 \to D^* pK$ is used (backup)

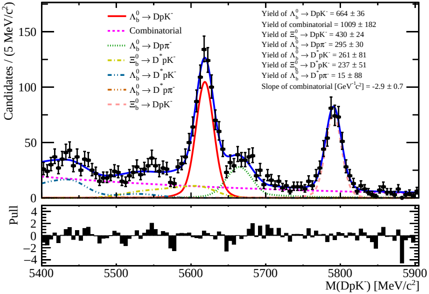

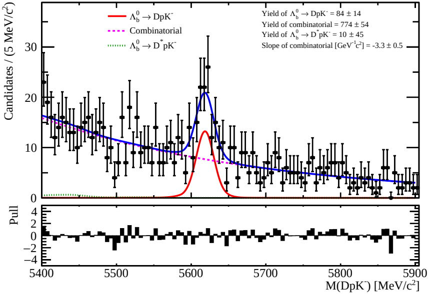

$$R = 8.55 \pm 1.47(\text{stat.})^{+0.38}_{-0.33}(\text{syst.})$$

$$A = 0.01 \pm 0.16(\text{stat.})^{+0.026}_{-0.024}(\text{syst.})$$

Systematic uncertainties in full phase space: summary

	R	A
Central value	7.14	0.119
Central value w/o efficiency correction	5.97	0.101
Statistical uncertainty	± 0.79	± 0.088
Systematic uncertainties		
fit model	$^{+0.37}_{-0.15}$	$^{+0.000}_{-0.011}$
efficiency corrections	$^{+0.21}_{-0.24}$	$^{+0.010}_{-0.008}$
PID	$^{+0.08}_{-0.16}$	$^{+0.001}_{-0.002}$
charmless background	± 0.08	
double misID background	± 0.005	
single misID background	± 0.001	
L0 TOS trigger efficiency	± 0.03	± 0.001
Λ_b^0 production asymmetry		± 0.015
p detection asymmetry		± 0.015
π detection asymmetry		± 0.005
Total systematic uncertainty	$^{+0.43}_{-0.33}$	$^{+0.024}_{-0.026}$

Systematic uncertainties in restricted phase space: summary

	$R_{M^2(pK^-)<5\,\mathrm{GeV}^2/c^4}$	$A_{M^2(pK^-)<5\,\mathrm{GeV}^2/c^4}$
Central value	8.55	0.007
Statistical uncertainty	±1.47	±0.158
Systematic uncertainties		
fit model	$^{+0.27}_{-0.02}$	$^{+0.011}_{-0.007}$
efficiency corrections	$^{+0.25}_{-0.28}$	$^{+0.010}_{-0.008}$
PID	$^{+0.09}_{-0.19}$	$^{+0.001}_{-0.002}$
charmless background	±0.10	
double misID background	±0.006	
single misID background	±0.001	
L0 TOS trigger efficiency	±0.03	±0.001
Λ_b^0 production asymmetry		±0.015
p detection asymmetry		±0.015
π detection asymmetry		±0.005
Total systematic uncertainty	$^{+0.38}_{-0.33}$	$^{+0.026}_{-0.024}$